



ELSEVIER

Journal of Chromatography A, 922 (2001) 25–36

JOURNAL OF  
CHROMATOGRAPHY A

www.elsevier.com/locate/chroma

# Estimation of width of narrow molecular-weight distributions by size-exclusion chromatography with concentration and light scattering detection

Miloš Netopilík<sup>a,\*</sup>, Štěpán Podzimek<sup>b</sup>, Pavel Kratochvíl<sup>a</sup>

<sup>a</sup>*Institute of Macromolecular Chemistry, Academy of Sciences of the Czech Republic, 162 06 Prague 6, Czech Republic*

<sup>b</sup>*SYNPO, 532 07 Pardubice, Czech Republic*

Received 29 December 2000; received in revised form 3 May 2001; accepted 8 May 2001

## Abstract

A new method for the estimation of the weight-to-number-average molecular-weight ratio,  $\bar{M}_w/\bar{M}_n$ , of polymers with a narrow molecular-weight distribution, approximated by log-normal distribution, is proposed using size-exclusion chromatography (SEC) with concentration and light-scattering detectors. From experimental data, the  $\bar{M}_w/\bar{M}_n$  ratios are calculated by two procedures: one using the concentration and light-scattering elution curve for the polymer measured, and the other based on the concentration elution curve and calibration line for a wide range of molecular masses. An iteration method has been developed making the two  $\bar{M}_w/\bar{M}_n$  ratios converge. The method was applied to a series of narrow molecular-weight distribution polystyrene standards. © 2001 Elsevier Science B.V. All rights reserved.

**Keywords:** Molecular mass distribution; Light scattering detection; Peak broadening; Polydispersity; Dual detection

## 1. Introduction

There are two major sources of error in the evaluation of size-exclusion chromatography (SEC) measurements on broad molecular-weight distribution (MWD) samples with simultaneous use of a concentration and a molecular-weight-sensitive detector: the peak broadening causing local polydispersity [1–6], and the error due to the decrease in the signal-to-noise ratio in both marginal parts of dual elution curves [5]. Both phenomena deteriorate the accuracy of the determination of the local molecular

mass [2]. The effect of peak (band) broadening, manifesting itself by a change of the slope of the dependence of molecular mass on elution volume, on the experimental values of molecular-weight averages, depends on the way of detection. In general, the significance of the peak broadening increases with decreasing polymer non-uniformity. With narrow MWD samples, a third problem, viz. that of exact value of the interdetector volume, complicates the situation still more [7–10]. The determination of non-uniformity of polymers with a narrow MWD is a topical problem enhanced by the fact that there is no reliable absolute method for the determination of the number-average molecular mass,  $\bar{M}_n$ , of polymers with high molecular mass.

For the dual light scattering/concentration detec-

\*Corresponding author. Tel.: +420-2-2040-3296; fax: +420-2-3535-7981.

E-mail address: netopil@imc.cas.cz (M. Netopilík).

tion, the weight-average molecular mass of the whole polymer,  $\bar{M}_w$ , is not directly affected by the peak broadening [2–6].

The determination of  $\bar{M}_n$  with an on-line light-scattering detector is complicated for several reasons: unlike  $\bar{M}_w$ ,  $\bar{M}_n$  is not invariant to peak broadening. The signal-to-noise ratio of the light-scattering detector is particularly unfavorable at the low-molecular-weight end of the elution curve, this part of the curve being crucial in the calculation of  $\bar{M}_n$  [5]. It has been shown [11] that, in calculations of weight and number averages of molecular masses for whole polymers from data for fractions, corresponding molecular-weight averages for fractions must be used. In SEC measurements with dual light scattering/concentration detection, however, only  $\bar{M}_w$  values for fractions are available.

For the characterization using dual light scattering/concentration detection of narrow-MWD samples, precise determination of the interdetector volume is absolutely essential [12–17]. Therefore, the effect of an error in the determination of the interdetector volume on the slope of the local calibration (i.e. that constructed from the data obtained in a dual light scattering/concentration detection SEC analysis of one sample) and MWD obtained is analyzed.

For polymers with narrow molecular-weight distribution, advantage can be taken of the fact that very often the elution curves may be approximated by a Gaussian curve which means that the MWD of the polymer is close to the log-normal distribution [18].

The use of this type of distribution is convenient and justified in cases where the broadness of the spreading function [19], which is a measure of peak broadening, is not negligible with respect to that of the experimental chromatogram and where both functions are Gaussian. The first condition is met if the extent of peak broadening is large or if sample non-uniformity is very low ( $\bar{M}_w/\bar{M}_n \rightarrow 1$ ). In both cases, the use of any discrete correction method is not reliable because the relative extent of the correction is large and the discrete numerical correction procedures tend to instability [20]. For this reason, assumptions about MWD are made and the elution curves are fitted by analytical functions [21].

In this paper, a new method of determination of the  $\bar{M}_w/\bar{M}_n$  ratio for polymers with narrow MWD by SEC with dual light scattering/concentration detec-

tion is proposed. It is based on assessing the extent of peak broadening by combination of its estimates obtained using the local (one-sample) calibration and calibration in a wide range of molecular masses.

## 2. Theory

With the dual light scattering/concentration detection, the experimental value of the weight-average molecular mass,  $\bar{M}_w$ , is independent of the peak broadening and its determination is facilitated by the fact that it can be obtained by integration of the light-scattering-peak area without combining light-scattering and concentration signals [2,3,6]. The determination of the  $\bar{M}_w/\bar{M}_n$  ratio for a sample with a MWD which can be approximated by the log-normal MWD is described in the following.

For samples with narrow MWD, the concentration elution curve can be approximated by a Gaussian curve [19]:

$$F(V) = \frac{1}{\sqrt{\pi}\sqrt{2\sigma^2 + \beta^2/B^2}} \exp\left[-\frac{(V_0 - V)^2}{2\sigma^2 + \beta^2/B^2}\right] \quad (1)$$

where  $V$  is the elution volume and  $V_0$  is the abscissa of the maximum:

$$\beta^2 = 2 \ln \bar{M}_w/\bar{M}_n \quad (2)$$

and  $B$  is the slope of the calibration dependence:

$$\ln M = A + BV \quad (3)$$

for a broad range of molecular masses, and thus not influenced by the peak broadening, and  $\sigma^2$  is variance of the spreading function [19] which is a measure of chromatographic peak broadening.

For  $\sigma^2 = 0$  in Eq. (1), the hypothetical curve:

$$W(V) = \frac{B}{\beta\sqrt{\pi}} \exp\left[-\frac{B^2}{\beta^2}(V_0 - V)^2\right] \quad (4)$$

corresponding to the log-normal MWD and no peak broadening results. Because of the effect of increasing peak broadening, the non-uniformity obtained from the detector data decreases on the contrary with broadening of the elution curve. The reason is the decrease in the slope of the local experimental

calibration,  $B_d$ , obtained in each measurement [22–26]. Its value with respect to the correct slope,  $B$ , defined by Eq. (3), is given by [27]:

$$B_d = B(\Sigma + \Delta/2) \quad (5)$$

where:

$$\Sigma = \beta^2 / (2\sigma^2 B^2 + \beta^2) \quad (6)$$

and:

$$\Delta = 4\delta B / (2\sigma^2 B^2 + \beta^2) \quad (7)$$

where  $\delta$  is a shift of the LS elution curve due to an error in the interdetector volume. With correct interdetector volume,  $\delta = 0$  and  $\Delta = 0$ ; if there is a negative error,  $\delta < 0$  (shift of the LS elution curve with respect to its correct position towards lower values of  $V$ , i.e. increased distance between LS and concentration elution curves),  $\Delta > 0$  (because  $B < 0$ ) and  $B_d$  increases and vice versa.

The usual practice to determine the interdetector volume is [13] aligning the concentration and LS elution curves of a narrow-MWD sample. Doubts may arise when the MWD width of that sample is close to the width of the analyzed one because the shift of the two elution curves for the sample used for the determination of the interdetector volume, due to its MWD width, however minute, cannot be, in principle, neglected. As the slope of local calibration,  $B_d$ , is affected by  $\delta$ , the comparison of its value with an independently determined value, is a good criterion of the correctness of the value of interdetector volume used in the calculations. This will be demonstrated in the Results and discussion section.

The relation between the apparent weight-to-number-average molecular-weight ratio,  $(\overline{M}_w/\overline{M}_n)_d$ , obtained from the detector data, and its true value,  $\overline{M}_w/\overline{M}_n$ , can be derived, e.g. as follows: The term  $2\sigma^2 + \beta^2/B^2$  in Eq. (1) is equivalent to the term  $\beta^2/B^2$  in Eq. (4), provided that the term  $\beta^2/B^2$  contains the apparent values  $\beta_d$  and  $B_d$ , i.e.,

$$\beta_d^2/B_d^2 = 2\sigma^2 + \beta^2/B^2 \quad (8)$$

where:

$$\beta_d^2 = 2 \ln(\overline{M}_w/\overline{M}_n)_d \quad (9)$$

The two ratios are related [10,27] by equation:

$$(\overline{M}_w/\overline{M}_n)_d = (\overline{M}_w/\overline{M}_n)^{\Sigma + \Delta} \exp Z \quad (10)$$

where the presence of  $\Delta$  and:

$$Z = 2(\delta B)^2 / (2\sigma^2 B^2 + \beta^2) \quad (11)$$

follows from a detailed analysis including the effect of  $\delta$  (cf. Eq. (36) of Ref. [10]).

On the other hand, the  $\overline{M}_w/\overline{M}_n$  ratio obtained from the combination of the concentration elution curve and calibration (3),  $(\overline{M}_w/\overline{M}_n)_c$ , calculated using an analogous procedure as in derivation of Eq. (10), i.e. putting:

$$\beta_c^2/B^2 = 2\sigma^2 + \beta^2/B^2 \quad (12)$$

is higher than the true ratio [28,29]:

$$(\overline{M}_w/\overline{M}_n)_c = (\overline{M}_w/\overline{M}_n) \exp(\sigma^2 B^2) \quad (13)$$

Eq. (13) has been derived regardless of any assumption concerning the polymer MWD. It has an alternative form [10,27] (see Appendix A and note in Ref. [30]):

$$(\overline{M}_w/\overline{M}_n)_c = (\overline{M}_w/\overline{M}_n)^{1/\Sigma} \quad (14)$$

which demonstrates that the change in the slope of the local calibration and in the  $\overline{M}_w/\overline{M}_n$  ratio experimentally found from the dual detection data is affected by the same factor  $\Sigma$ .

In the following theoretical treatment, it is assumed that  $\delta = 0$ . In the Results and discussion section, a potential error due to  $\delta \neq 0$  is estimated and a procedure for checking the correct value of interdetector volume, i.e.  $\delta \rightarrow 0$  is proposed.

For illustration, Fig. 1 presents the  $\overline{M}_w/\overline{M}_n$  ratios, calculated according to Eqs. (10) and (13) or (14) for the calibration dependence:

$$\log M = 12.2 - 0.415V \quad (15)$$

and  $\overline{M}_w/\overline{M}_n = 1.1, 1.5$  and  $2$ .

Eqs. (10) and (13) or (14), and Fig. 1 indicate that the true  $\overline{M}_w/\overline{M}_n$  ratio is between the two experimental ones, i.e.  $(\overline{M}_w/\overline{M}_n)_d < \overline{M}_w/\overline{M}_n < (\overline{M}_w/\overline{M}_n)_c$ . Hence, the corrected value of  $\overline{M}_w/\overline{M}_n$ , which is the best achievable approximation to the true value, can be found by correcting the light scattering and concentration elution curves to the extent that the  $(\overline{M}_w/\overline{M}_n)_d$  value, calculated by combination of the concentration elution curve and  $M$  determined from

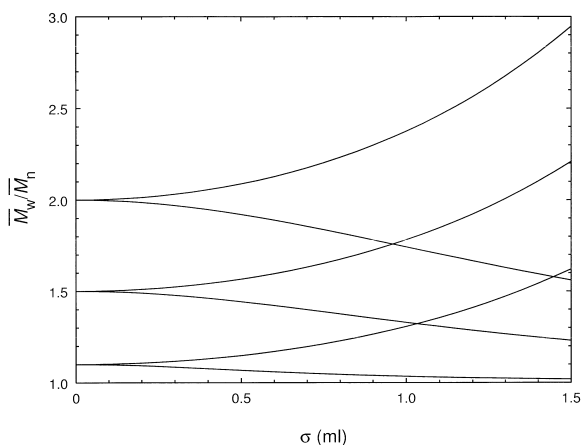


Fig. 1. The dependences on the variance,  $\sigma$ , of the  $\overline{M}_w/\overline{M}_n$  ratios determined from the combination of concentration elution curves and calibration in a broad range of molecular masses (calculated according to Eqs. (13) or (14), rising curves) and from the dual-detection light scattering/concentration (calculated according to Eq. (10), descending curves) for calibration given by Eq. (15) and  $\overline{M}_w/\overline{M}_n = 1.1, 1.5$  and  $2$  (values at  $\sigma = 0$ ).

calibration obtained from combination of light scattering and concentration elution curves for one sample, and the  $(\overline{M}_w/\overline{M}_n)_c$  value, determined from the concentration elution curve and calibration in a wide range of molecular masses, match. The advantage of this approach consists in the fact that for narrow MWD samples the values of  $(\overline{M}_w/\overline{M}_n)_c$  are close to  $(\overline{M}_w/\overline{M}_n)_d$  and thus the possible error in finding the best approximation to the true value of  $\overline{M}_w/\overline{M}_n$ , situated between the two experimental ones, decreases with decreasing sample non-uniformity.

For a polymer with log-normal MWD, the procedure of finding the corrected  $\overline{M}_w/\overline{M}_n$  is based on combination of Eqs. (10) and (13) or (14). The value of  $\sigma^2$  can be found (cf. Appendix B) by an iteration procedure using the formula:

$$\sigma_{i+1}^2 = \frac{E - \beta_c^2 + 2\sigma_i^2 B^2 + \sqrt{(\beta_c^2 - 2\sigma_i^2 B^2)^2 + E^2}}{2B} \quad (16)$$

where:

$$E = \ln [(\overline{M}_w/\overline{M}_n)_c / (\overline{M}_w/\overline{M}_n)_d] \quad (17)$$

The resulting value of  $\sigma^2 \equiv \sigma_\infty^2$  is then used for calculation of  $\overline{M}_n$  according to Eq. (13) as:

$$\overline{M}_n = \overline{M}_w (\overline{M}_w/\overline{M}_n)_c^{-1} \exp(\sigma^2 B^2) \quad (18)$$

### 3. Experimental

SEC measurements with dual light scattering/concentration detection were performed using the Waters set (Pump 600, autosampler 717, differential refractometer 410, two columns Styragel HR 5E 300  $\times$  7.8 mm, particle size 7–10  $\mu\text{m}$ . Mixed separating in the range approximately 1000–2 000 000 g/mol). The set was connected to a scattering photometer miniDAWN (Wyatt Technology Corp.).

The data were accumulated and processed using the Wyatt Technology ASTRA Software for Windows and some calculations were performed using home-modified software.

The interdetector volume 0.183 ml found in the first approximation using the Astra Software by aligning the concentration and LS elution curves of a narrow-MWD sample ( $\overline{M}_w = 2 \times 10^5$ ) was checked independently as described in the Results and discussion section.

Ten polystyrene narrow-MWD standards, with molecular masses in the range  $1.9 \times 10^4$ – $4.34 \times 10^6$ , and one sample (a) with broader MWD were used in the experiments (Table 1). Standards of molecular masses  $\overline{M}_w \times 10^{-3} = 19, 90$  and  $200$  (the values given by the producer) are from Pressure Chemical, the rest from Polymer Laboratories.

Correction of the light-scattering data for finite concentration was made by the Astra Software using the values of the second virial coefficient,  $A_2$ , (Table 1) calculated according to equation [31]:

$$A_2 = 0.01 \times M^{-0.25} \quad (19)$$

The dependences of  $\log M$  vs.  $V$  in the central linear region (Fig. 2), where the concentration is high enough to determine  $M$  reliably, were graphically fitted by a line with abscissa and slope  $A_{d,10}$  and  $B_{d,10}$ , respectively, where the subscript “10” denotes the use of logarithm to base 10 in constructing the local calibration (cf. Eq. (3)). This notation will be used in the following in discussing experimental

Table 1

The results of SEC dual-detector analysis of polystyrene standards denoted with nominal molecular mass in thousands and broad-MWD polystyrene sample *a*: weight-average molecular mass,  $\bar{M}_w$ , second virial coefficient,  $A_2$ , slope  $B_{d,10}$  of the dependence of  $\log M$  vs.  $V$  from one-sample analysis, variance of the spreading function,  $\sigma^2$ , values of  $\bar{M}_w/\bar{M}_n$  ratio given by the producer (subscript “p”), obtained using local calibration from detector data in one analysis (subscript “d”), using calibration in a broad range of elution volume (subscript “c”) and corrected for peak broadening (no subscript); The standards are identified by molecular masses, in thousands, given by the producer

Sample	$A_2 \times 10^4$ mol $\times$ ml/g <sup>2</sup>	$\bar{M}_w \times 10^{-3}$	$-B_{d,10}$ ml <sup>-1</sup>	$\sigma$ ml	$(\bar{M}_w/\bar{M}_n)_p$	$(\bar{M}_w/\bar{M}_n)_d$	$(\bar{M}_w/\bar{M}_n)_c$	$\bar{M}_w/\bar{M}_n$
19	8.4	19.1	0.070	0.298	1.03	1.0028	1.1030	1.0167
90	5.8	89.1	0.046	0.270	1.04	1.0009	1.0779	1.0083
200	4.7	214.3	0.027	0.254	1.05	1.0003	1.0652	1.0042
310	4.2	317.5	0.034	0.282	1.05	1.0005	1.0825	1.0065
470	3.8	468.8	0.022	0.333	1.08	1.0003	1.1130	1.0058
675	3.5	659.1	0.082	0.309	1.07	1.0042	1.1152	1.0216
1020	3.1	1040	0.030	0.325	1.08	1.0006	1.1103	1.0076
1840	2.7	1791	0.104	0.274	1.06	1.0057	1.0955	1.0229
2850	2.4	2912	0.061	0.344	1.08	1.0027	1.1348	1.0186
4340	2.2	4653	0.078	0.336	1.06	1.0044	1.1352	1.0239
<i>a</i>	4.3	320	0.350	0.346		2.2180	2.7289	2.4450

local calibrations. The elution volume  $V_w$  corresponding to  $\bar{M}_w$  of individual samples was then calculated (cf. Eq. (3)) as [32]:

$$V_w = \frac{\log \bar{M}_w - A_{10}}{B_{10}} \quad (20)$$

The values of  $V_w$  were used for the construction of the wide-range calibration (Eq. (15), Fig. 3) and further calculations.

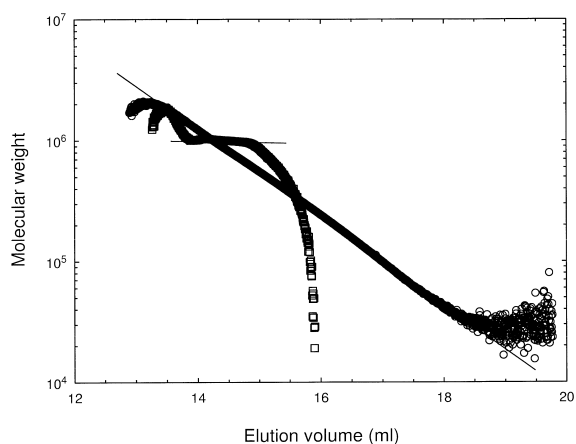


Fig. 2. Comparison of dependences of  $\log M$  vs. elution volume obtained from the dual elution curves for a standard  $\bar{M}_p = 1020 \times 10^3$  ( $\square$ ) and sample *a* ( $\circ$ ).

#### 4. Results and discussion

The concentration and light scattering elution curves, the latter extrapolated to zero angle and concentration [33], of narrow standards are symmetrical and Gaussian-shaped (an example is given in Fig. 4) which justifies the use of the procedures based on the approximation of MWD by the log-normal function. The shapes of the elution curves for sample *a* with broader MWD are somewhat less symmetrical; hence the results discussed

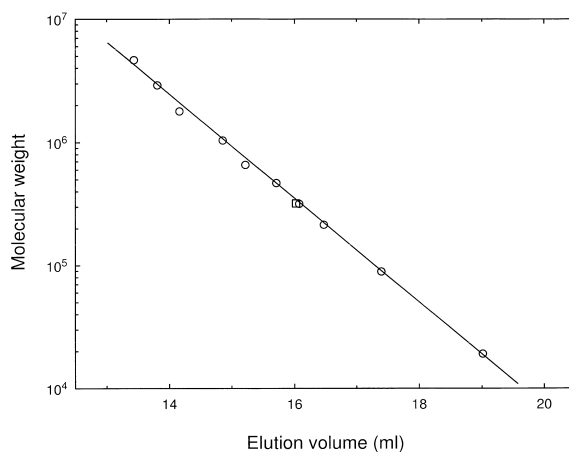


Fig. 3. The dependence of weight-average molecular mass on elution volume (Eq. (15)) obtained for polystyrene standards ( $\circ$ ) and sample *a* ( $\square$ ).

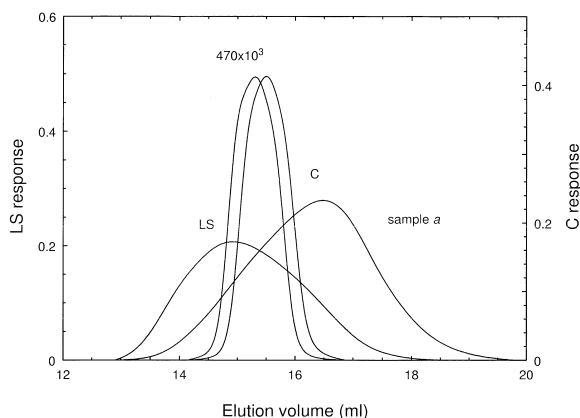


Fig. 4. Typical example of a dual light scattering/concentration detection SEC analysis: Comparison of the unnormalized concentration (C) and light scattering (LS) (extrapolated to zero angle and concentration) elution curves for a narrow-MWD standard  $\bar{M}_n \times 10^{-3} = 470$  and broad-MWD sample *a* (denoted with the curves).

for this sample refer to an implicit polymer with the same  $\bar{M}_w$  and  $\bar{M}_w/\bar{M}_n$  but with a perfectly Gaussian peak. Also, there are some deviations in the tails of the elution curves. Nevertheless, the dependences of  $\log M$  vs.  $V$  for both sample *a* and narrow-MWD standards in the central region can be fitted by straight lines (Fig. 2) from which the abscissas and slopes,  $A_{d,10}$  and  $B_{d,10}$ , are determined and the elution volume  $V_w$  is found according to Eq. (20). For the present set of samples, the calibration dependence (15) results (Fig. 3).

It is pertinent to analyse the effect of potential error in the determination of the interdetector volume on the values of  $B_d$  and  $\bar{M}_w/\bar{M}_n$ . Fig. 5a and b present the dependences of ratio  $B_d/B$  of the slopes of local to long-range calibrations on  $\delta$ , calculated according to Eq. (5), respectively, for  $\sigma = 0$  and 0.3 ml, a value close to the experimental ones (cf. Table 1). It can be seen that  $B_d$  is sensitive to  $\delta$  and this sensitivity increases at  $\bar{M}_w/\bar{M}_n \rightarrow 1$ . As can be expected, the effect for the experimental values  $\sigma \approx 0.3$  ml is lower. On the other hand, the corresponding change in  $(\bar{M}_w/\bar{M}_n)_d$ , calculated according to Eq. (10), is depressed even for  $\sigma = 0$ ; one can see (Fig. 6) that  $(\bar{M}_w/\bar{M}_n)_d$  is in the limits usually taken for a good precision even if  $B_d$  changes dramatically. This is the theoretical proof of an experimentally established rule [26]. On the other hand, a reasonable

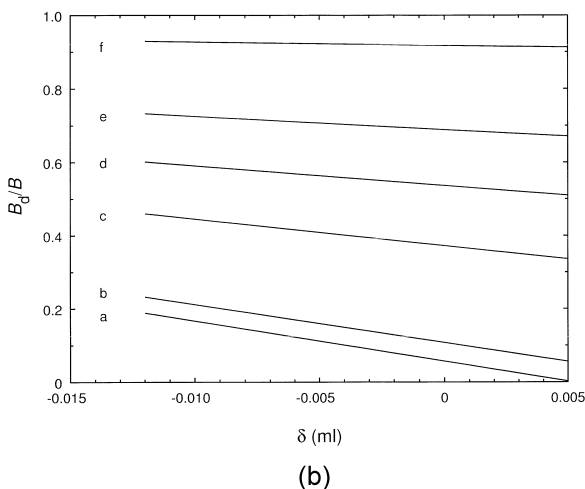
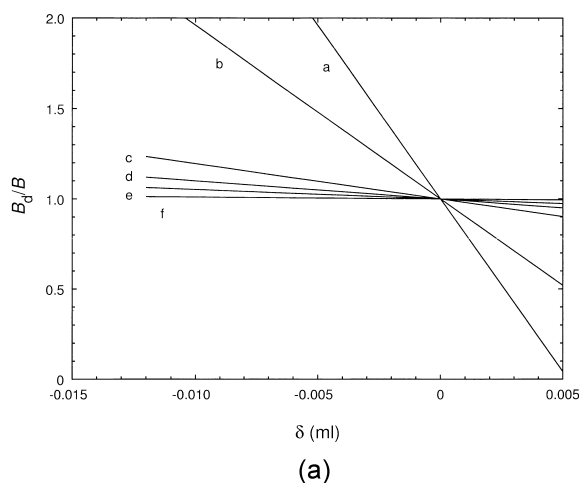


Fig. 5. The dependences of  $B_d/B$  for  $\bar{M}_w/\bar{M}_n = 1.005, 1.01, 1.05, 1.1, 1.2$  and  $2.5$  (curves “a” through “f”, respectively) on  $\delta$  calculated according to Eq. (5) for calibration given by Eq. (15) and (a) hypothetical case with no spreading ( $\sigma = 0$ ); (b) real case ( $\sigma = 0.3$  ml).

precision in the determination of  $B_d$  implicates a good precision in determination of  $(\bar{M}_w/\bar{M}_n)_d$ .

As the interdetector volume is often found from the distance of the maxima of the concentration and light-scattering elution curves of narrow-MWD samples, instead of uniform ones, it is worthwhile to check the error due to different MWD widths. For a sample with the log-normal MWD, the shift of the peak maximum of the LS elution curve with respect to the concentration curve due to the non-uniformity in  $M$  is  $\beta^2/2B$  [10]. Hence, when aligning the two

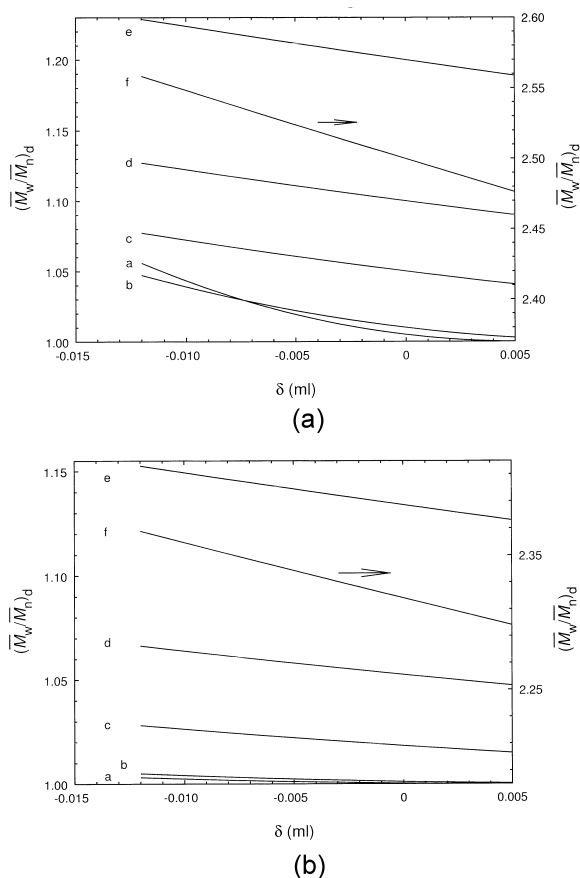


Fig. 6. The dependences of  $(\overline{M}_w/\overline{M}_n)_d$  on  $\delta$  (the same labeling of curves as in Fig. 5; the right-hand scales apply to curves “f” as denoted by arrows at the curves) calculated according to Eq. (5) for calibration given by Eq. (15) and (a) hypothetical case with no spreading ( $\sigma = 0$ ); (b) real case ( $\sigma = 0.3$  ml).

elution curves so that the elution volumes of maxima are identical, the positive (because  $B < 0$ ) error in the interdetector volume, caused by the shift of the LS elution curve towards the concentration signal is:

$$\delta = -\beta^2/2B \quad (21)$$

According to Eq. (21), the accuracy of the determination of the interdetector volume by alignment depends on weight-to-number average ratio,  $(\overline{M}_w/\overline{M}_n)_s$ , of the reference standard used. To illustrate the effect of  $(\overline{M}_w/\overline{M}_n)_s$  on the value of  $(\overline{M}_w/\overline{M}_n)_d$ , the dependences of  $(\overline{M}_w/\overline{M}_n)_d$  on the  $\overline{M}_w/\overline{M}_n$  ratio of the sample were computed for several values of

$(\overline{M}_w/\overline{M}_n)_s$  (curves in Fig. 7 are labeled with those values). In order to distinguish the effect caused by the peak broadening, the dependences were calculated for  $\sigma = 0$  (Fig. 7a and b) and for  $\sigma = 0.3$  ml (Fig. 7c and d), the value around which those experimentally obtained with our separation system (Table 1) fluctuate. The dependences are shown for a narrow and a broad MWD range (Fig. 7a, c and b, d, respectively). For  $\sigma = 0.3$  ml, the curves for the same  $(\overline{M}_w/\overline{M}_n)_s$  ratio are less steep than for  $\sigma = 0$ , but they follow approximately the same pattern. With increasing  $(\overline{M}_w/\overline{M}_n)_s$  ratios, the dependences of  $(\overline{M}_w/\overline{M}_n)_d$  on  $\overline{M}_w/\overline{M}_n$  deviate from the limiting dependence calculated for  $(\overline{M}_w/\overline{M}_n)_s = 1$  (i.e.  $\delta = 0$ ; the dependence is not shown in Fig. 7b and d because it almost coincides with the dependences for the ratio  $(\overline{M}_w/\overline{M}_n)_s = 1.001$ ). All dependences touch the  $\overline{M}_w/\overline{M}_n$  axis in the points  $\overline{M}_w/\overline{M}_n = (\overline{M}_w/\overline{M}_n)_s$  (and  $(\overline{M}_w/\overline{M}_n)_d = 1$ ) as follows from introducing Eq. (21) (with  $\beta^2$  given by Eq. (2) for  $\overline{M}_w/\overline{M}_n = (\overline{M}_w/\overline{M}_n)_s$ ) into Eq. (10). This can be understood also in another way: introducing Eq. (21) into Eq. (5) gives  $B_d = 0$  which implies  $(\overline{M}_w/\overline{M}_n)_d = 1$  even if the concentration elution curve has a finite broadness (because the same molecular mass is detected irrespectively of the elution volume). The parts of the curves rising with  $\overline{M}_w/\overline{M}_n \rightarrow 0$  correspond to the situation when  $\overline{M}_w/\overline{M}_n < (\overline{M}_w/\overline{M}_n)_s$  and  $B_d > 0$ , i.e. to analysis samples with a lower  $\overline{M}_w/\overline{M}_n$  ratio than that of those used for the determination of the interdetector volume. Although the situation with  $B_d > 0$  lacks physical meaning, it demonstrates that false but seemingly acceptable results can be obtained using an erroneous value of interdetector volume.

From Fig. 7c and d, the reliability of the determination of the interdetector volume for the characterization of narrow-MWD samples can be conveniently estimated in terms of the quantity  $(\overline{M}_w/\overline{M}_n)_d - 1$ . If extremely narrow-MWD samples of  $1.001 < (\overline{M}_w/\overline{M}_n)_s < 1.005$  are used for the determination of the interdetector volume, the expected error in terms of  $(\overline{M}_w/\overline{M}_n)_d - 1$  for a sample of  $\overline{M}_w/\overline{M}_n = 1.05$  is between 5 and 20% and it decreases with increasing  $\overline{M}_w/\overline{M}_n$  ratio of the sample. The values of the  $\overline{M}_w/\overline{M}_n$  ratio found for our standards are approximately in the range  $1.005 < (\overline{M}_w/\overline{M}_n)_s < 1.01$  which implies a maximum error in  $(\overline{M}_w/\overline{M}_n)_d - 1$  of

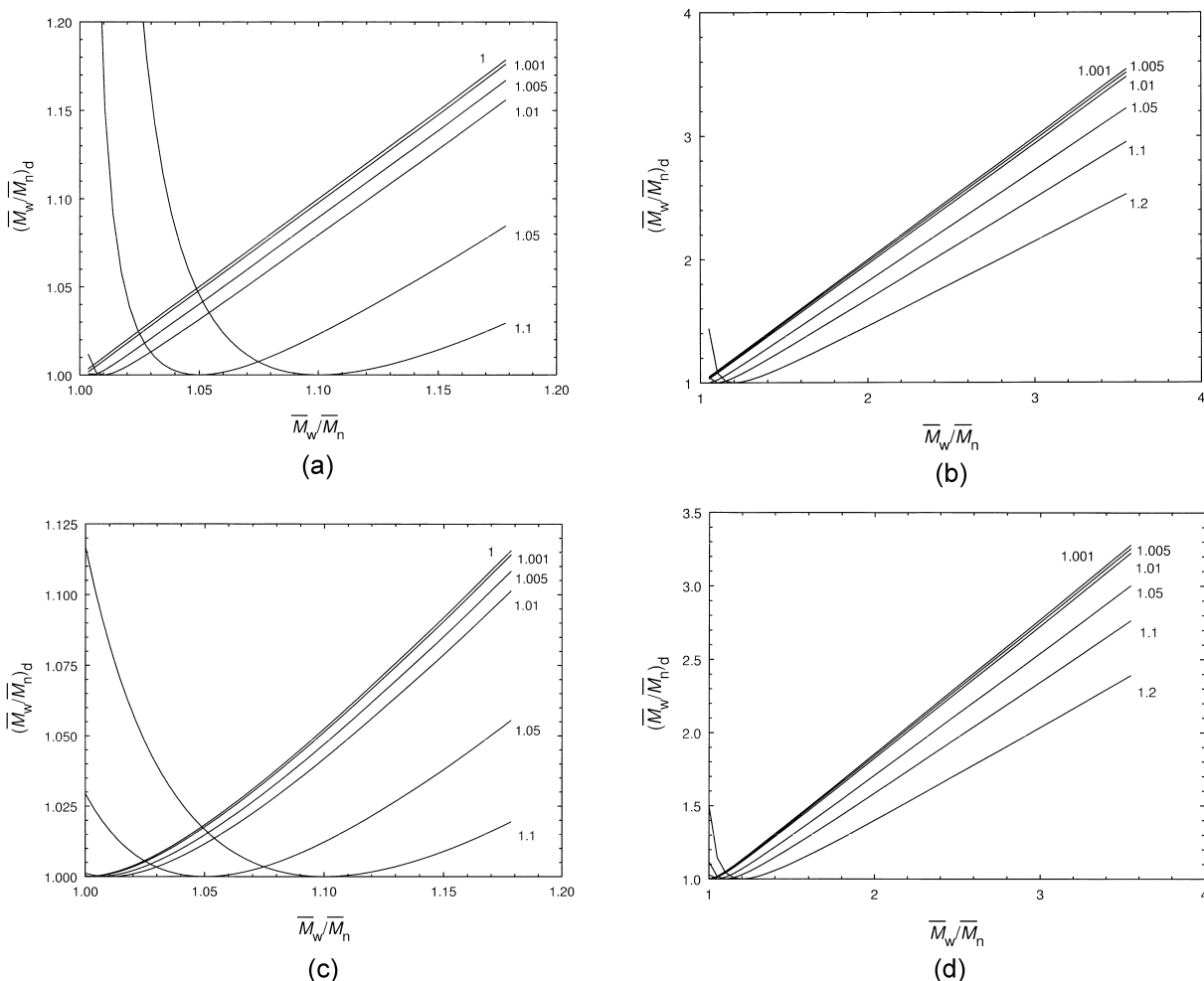


Fig. 7. The effect of the  $(\overline{M}_w/\overline{M}_n)_s$  ratio values labeling the curves of the reference standards used for the determination of the interdetector volume on the dependence of the ratio  $(\overline{M}_w/\overline{M}_n)_d$  on the true  $\overline{M}_w/\overline{M}_n$  of the samples analyzed;  $(\overline{M}_w/\overline{M}_n)_d$  was calculated from Eq. (10) using  $\delta$  values following from Eq. (21) for calibration given by Eq. (15) and (a)  $\sigma = 0$ , narrow range of  $\overline{M}_w/\overline{M}_n$ ; (b)  $\sigma = 0$ , broad range of  $\overline{M}_w/\overline{M}_n$ ; (c)  $\sigma = 0.3$  ml, narrow range of  $\overline{M}_w/\overline{M}_n$ ; (d)  $\sigma = 0.3$  ml, broad range of  $\overline{M}_w/\overline{M}_n$ .

8 to 16% for a sample with the ratio  $\overline{M}_w/\overline{M}_n = 1.15$ . This is a fair accuracy considering other sources of error occurring in the characterization of narrow-MWD samples [5]. As can be seen from Fig. 7d, for polymers with broad MWD, the effect of an error in the interdetector volume is negligible for  $(\overline{M}_w/\overline{M}_n)_s \leq 1.01$ . On the other hand, samples with the ratio  $(\overline{M}_w/\overline{M}_n)_s > 1.1$  should never be used for the interdetector volume determination because they are not reliable for any range of  $\overline{M}_w/\overline{M}_n$ .

The values of  $B_d$  determined for narrow-MWD

samples and the quantities calculated therefrom are subject to further discussion. Thus, it is worthwhile to check their values and also the correctness of the determination of the interdetector volume used for their calculation, by a procedure based on the signal from a single detector and thus independent of the interdetector volume. A method called z-detection, based on the determination of the root-mean-square radius of gyration,  $\langle s^2 \rangle^{1/2}$ , has been proposed [10] as an alternative way of determination of molecular mass which is calculated from the LS data only.



For our separation system and several standards in a range of  $470 < \overline{M}_w \times 10^{-3} < 4340$ , the relation between  $M$  and  $\langle s^2 \rangle^{1/2}$  described by equation:

$$\log M = 3.494 + 1.505 \log \langle s^2 \rangle^{1/2} \quad (22)$$

was obtained [34]. The molecular masses were calculated from the radii of gyration according to Eq. (22). In Fig. 8, the  $B_{d,10}$  values determined by the dual-detection method are plotted against those obtained by the z-detection. Although the scatter of points is rather large, there is no systematic deviation in  $B_{d,10}$  values obtained by the two methods. Thus, one can conclude that the error in the interdetector volume is negligible and need not be considered in the following discussion.

Table 1 lists the results of SEC analyses of ten narrow-MWD polystyrene standards, differing in molecular mass, and a broad-MWD sample *a*. The absolute values of the slopes  $B_{d,10}$  of local calibrations are lower than the slope for calibration (15) in a broad range of molecular masses (Fig. 3), which is in accord with both theory and observations of other authors [23–26]. As expected, the ratios  $(\overline{M}_w/\overline{M}_n)_d$  obtained from the dual-detector data (one-sample calibrations) are lower in comparison with the values of the ratio  $(\overline{M}_w/\overline{M}_n)_c$  obtained from the broad-range calibration and concentration detection. The broadness of the spreading function is expressed as standard deviation  $\sigma$  rather than variance  $\sigma^2$

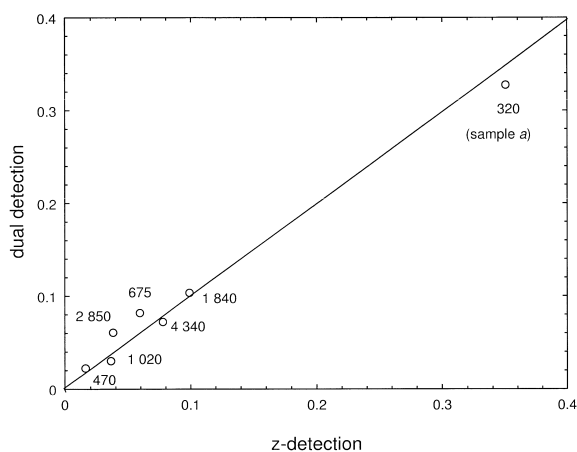


Fig. 8. Comparison of the values of  $B_{d,10}$  found by dual detection with those found by the z-detection for samples of molecular masses (in thousands) given with the points.

because of the geometrical meaning of  $\sigma$  as the approximate half-width in the half-height of a peak of a uniform polymer. The values of  $\sigma$  calculated according to Eq. (16) are scattered about 0.3 ml. The value of  $\sigma$  for the broad-MWD sample, although among the highest, is in the range of those obtained for the narrow-MWD samples.

The procedure of searching for the correct value of  $\sigma$  according to Eq. (16) and, through it, for  $\overline{M}_w/\overline{M}_n$  is graphically demonstrated in Fig. 9 for the narrow-MWD standard  $\overline{M}_w = 1020 \times 10^3$  and the broad-MWD sample *a*. The corrected values in this Figure,  $(\overline{M}_w/\overline{M}_n)_{c,corr}$ , were calculated using the equation:

$$(\overline{M}_w/\overline{M}_n)_{c,corr} = (\overline{M}_w/\overline{M}_n)_c \exp[-\sigma^2 B^2] \quad (23)$$

derived from Eq. (13) and denoting the values of  $(\overline{M}_w/\overline{M}_n)_c$  corrected by particular values of  $\sigma$  as  $(\overline{M}_w/\overline{M}_n)_{c,corr}$ .

Similarly, the corrected values of  $(\overline{M}_w/\overline{M}_n)_d$ ,  $(\overline{M}_w/\overline{M}_n)_{d,corr}$ , were calculated using the equation:

$$(\overline{M}_w/\overline{M}_n)_{d,corr} = (\overline{M}_w/\overline{M}_n)_d^{1/\Sigma_{corr}} \quad (24)$$

derived from Eq. (10); in Eq. (24),  $(\overline{M}_w/\overline{M}_n)_{d,corr}$  denotes the values of  $(\overline{M}_w/\overline{M}_n)_d$  corrected by a particular value of  $\sigma$ ;  $\Sigma_{corr}$  was calculated using the correct slope,  $B_{10} = -0.415 \text{ ml}^{-1}$ , of the calibration (cf. Eqs. (3) and (15)) according to Eq. (6) as:

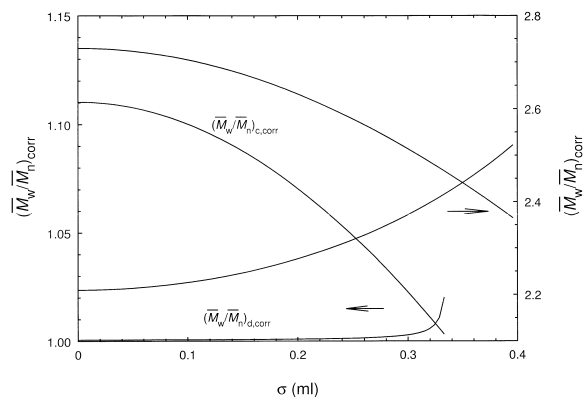


Fig. 9. Comparison of the dependences on standard deviation  $\sigma$  of the corrected ratios  $(\overline{M}_w/\overline{M}_n)_{c,corr}$ , referring to the combination of the concentration elution curve and the broad-range calibration, with  $(\overline{M}_w/\overline{M}_n)_{d,corr}$ , referring to the light scattering/concentration dual-detection, calculated, respectively, according to Eqs. (23) and (24). Examples: a narrow-MWD standard ( $\overline{M}_p = 1020 \times 10^3$ , Table 1, left scale) and the broad-MWD sample *a* (right scale).

$$\Sigma_{\text{corr}} = \frac{\beta_{\text{c,corr}}^2/B^2}{2\sigma^2 + \beta_{\text{c,corr}}^2/B^2} \quad (25)$$

where  $\beta_{\text{c,corr}}$  was calculated using Eq. (12) as:

$$\beta_{\text{c,corr}}^2 = \beta_{\text{c}}^2 - 2\sigma^2 B^2 \quad (26)$$

where  $\beta_{\text{c}}^2 = 2 \ln(\overline{M}_w/\overline{M}_n)_c$ .

From Fig. 9 it can be seen that the dependence of  $(\overline{M}_w/\overline{M}_n)_{\text{c,corr}}$  on  $\sigma$  calculated according to Eq. (23) for a narrow-MWD standard decreases gradually while the values of  $(\overline{M}_w/\overline{M}_n)_{\text{d,corr}}$  change only slightly almost in the whole range but they start to increase abruptly in a close vicinity of the intersection. For the broad-MWD sample *a*, the extent of the change in  $(\overline{M}_w/\overline{M}_n)_{\text{c,corr}}$  is virtually the same as in  $(\overline{M}_w/\overline{M}_n)_{\text{d,corr}}$ , both curves being nearly symmetrical, and the corrected value of  $(\overline{M}_w/\overline{M}_n)_{\text{corr}}$  is almost the average of the two experimental ones.

The best approximations to the correct values of  $\overline{M}_w/\overline{M}_n$  and  $\sigma$  (resulting also from the iteration procedure according to Eq. (16)) are found at the intersection of both curves.

For values of  $\sigma$  higher than the end of the curves in Fig. 9, the values of  $\beta_{\text{c,corr}}$  calculated according to Eq. (26) are negative and unrealistic values of  $\overline{M}_w/\overline{M}_n < 1$  result. This should be kept in mind when choosing the initial values of  $\sigma$  for the iteration procedure according to Eq. (16).

The slopes,  $B_{\text{d},10}$ , were determined graphically from the straight lines fitted through the points corresponding to the central parts of the concentration elution curves. As the local calibrations are linear in their central parts (Fig. 2), the determination could be done with a good precision. For the narrow-MWD samples, however, the slopes are very close to their limiting value for a large peak broadening (Fig. 2),  $B_{\text{d},10} \rightarrow 0$ . Consequently, small errors in the determination of the slopes may cause large errors in the calculated values of  $\sigma$  (Table 1). The large experimental error in  $\sigma$  is one of many manifestations in solutions to the “ill-posed” problems. For this reason, a reliable analysis of this problem has to be done on a large set of samples. The value found for sample *a*, although among the highest, differs from that found for standards of  $\overline{M}_w \times 10^{-6} = 2.85$  and 4.34, by less than 3% which is below the experimental error.

The presence of the highest values of  $\sigma$  in the range of high molecular masses seems to suggest an increase in  $\sigma$  with  $M$ . This is in accord with the observation of other authors [13,29,35,36]. Fig. 5 in a paper by Cheung et al. [13] presents the dependence of  $\sigma$  on  $M$ , found for a series of polystyrene standards, starting with values of  $\sigma \approx 0.3$  ml at low  $M$  (in accord with our measurements), rising slowly with  $M$  to  $\sigma \approx 0.6$  ml for  $M \approx 10^6$  and then, for one sample, abruptly to  $\sigma \approx 1.4$  ml for  $M$  in the order of millions. Such a dramatic increase of  $\sigma$  with  $M$ , however, was not observed in our experiments. The origin of increased values of  $\sigma$  has to be sought in the effect of increased viscosity of solutions due to high molecular mass and/or concentration because the interaction of high-molecular mass samples with solid-phase is small [37].

It is interesting to compare the values of the  $\overline{M}_w/\overline{M}_n$  ratio with its limits imposed by the theory of polymerization without termination [38]. In the limiting case when all chains start growing simultaneously and no reaction of polymer with polymer occurs, the MWD of the polymer is given by the Poisson distribution and:

$$\overline{M}_w = M_0(\nu^2 + 3\nu + 1)/(\nu + 1) \quad (27)$$

and:

$$\overline{M}_n = M_0(\nu + 1) \quad (28)$$

where  $\nu$  is the kinetic chain length and  $M_0$  is the molecular mass of a monomeric unit. Then:

$$\overline{M}_w/\overline{M}_n = 1 + \nu/(\nu + 1)^2 \quad (29)$$

Fig. 10 presents a comparison of the dependence of  $\overline{M}_w/\overline{M}_n$  on  $\overline{M}_w$ , calculated according to Eqs. (27) and (29), with the experimental values from Table 1. It can be seen that all values, except one, are situated above the curve for the Poisson distribution. The value of  $(\overline{M}_w/\overline{M}_n)_d$  for the standard  $\overline{M}_p \times 10^{-3} = 19$  is somewhat below the curve, which can be explained by the hypothesis that the values of  $(\overline{M}_w/\overline{M}_n)_d$  are lower than the correct ones (cf. Fig. 9). On the other hand, the corrected  $\overline{M}_w/\overline{M}_n$  ratios are situated in the vicinity of the curve for the Poisson distribution. The values of  $(\overline{M}_w/\overline{M}_n)_c$  are systematically somewhat higher than those given by the producer,  $(\overline{M}_w/\overline{M}_n)_p$ . The corrected  $\overline{M}_w/\overline{M}_n$  ratio, lower than the values given by the producer,  $(\overline{M}_w/\overline{M}_n)$

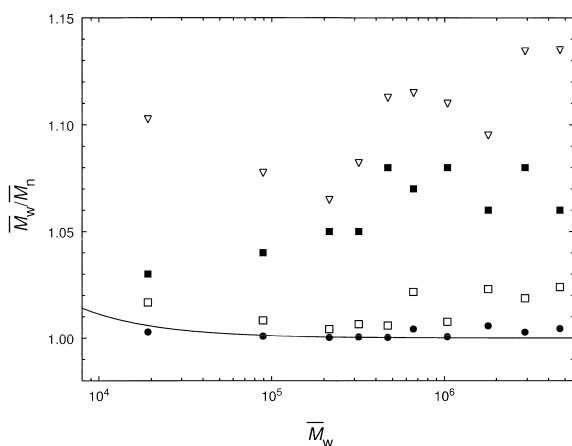


Fig. 10. Comparison of the  $\bar{M}_w/\bar{M}_n$  ratios in dependence on weight-average molecular mass,  $\bar{M}_w$ , with the dependence calculated according to Eqs. (27) and (29) (full line). Data points: values given by the producer (■),  $(\bar{M}_w/\bar{M}_n)_c$  (▽),  $(\bar{M}_w/\bar{M}_n)_d$  (●),  $\bar{M}_w/\bar{M}_n$  values corrected by the present method (□).

$\bar{M}_n)_p$ , is between the two experimental values, as expected from Eqs. (10) and (13) (or (14)). The lower is the value of  $(\bar{M}_w/\bar{M}_n)_d$  the closer is the corrected value of  $\bar{M}_w/\bar{M}_n$  (and the more distant is this value from  $(\bar{M}_w/\bar{M}_n)_c$ ). Out of the uncorrected values, however, the  $(\bar{M}_w/\bar{M}_n)_d$  ratios are better approximations to the corrected  $\bar{M}_w/\bar{M}_n$  ratios.

## 5. Conclusions

(1) The  $\bar{M}_w/\bar{M}_n$  ratio determined by SEC analysis of one polymer with concentration and light-scattering detection,  $(\bar{M}_w/\bar{M}_n)_d$ , is lower than the  $(\bar{M}_w/\bar{M}_n)_c$  ratio obtained using calibration in a wide range of  $M$  and concentration detection. The correct value of  $\bar{M}_w/\bar{M}_n$  is between the two experimental values, i.e.  $(\bar{M}_w/\bar{M}_n)_d < \bar{M}_w/\bar{M}_n < (\bar{M}_w/\bar{M}_n)_c$ .

(2) A method for finding the extent of peak broadening from dual light-scattering/concentration record is demonstrated for samples with the log-normal MWD. The method is based on combining the ratio  $(\bar{M}_w/\bar{M}_n)_d$ , obtained from the dual record, and the  $(\bar{M}_w/\bar{M}_n)_c$  ratio, obtained from the concentration record and the calibration by several narrow-MWD samples in a broad range of molecular masses. As, for narrow-MWD samples, the two experimental ratios approach each other, the possible

error in finding the best approximation to the true value of  $\bar{M}_w/\bar{M}_n$  decreases with decreasing width of MWD, provided the slope of the experimental dependence of  $\log M$  vs.  $V$  is reliably determined.

(3) The effect of peak broadening on the experimental  $\bar{M}_w/\bar{M}_n$  ratio obtained from concentration elution curve and conventional calibration is larger than that on the  $\bar{M}_w/\bar{M}_n$  ratio obtained from measurement with light scattering/concentration dual-detection. Using an efficient separation system, the molecular masses obtained from uncorrected dual-detection data are a good approximation to correct values even for narrow-MWD samples.

(4) The interdetector volume found by aligning the LS and concentration elution curves for samples with the ratio  $1.005 < (\bar{M}_w/\bar{M}_n)_s < 1.01$  is determined with an accuracy ensuring the determination of the  $(\bar{M}_w/\bar{M}_n)_d$  ratio for samples with the ratio  $\bar{M}_w/\bar{M}_n = 1.15$ , with a maximum error, expressed in terms of the quantity  $(\bar{M}_w/\bar{M}_n)_d - 1$ , of 8 to 16%, decreasing with the  $\bar{M}_w/\bar{M}_n$  ratio of the sample. If narrow-MWD samples with, say,  $\bar{M}_w/\bar{M}_n < 1.15$  are characterized, it is advisable to check the interdetector volume by an independent method, e.g. that based on the z-detection.

(5) SEC measurements with the dual light scattering/concentration detection indicate that the ratios  $\bar{M}_w/\bar{M}_n$  of commercial standards may be lower than currently given by the producers and slightly higher than the assumed limit of Poisson distribution.

## Acknowledgements

The authors gratefully acknowledge the temporary loan of a miniDAWN laser photometer from Wyatt Technologies Ltd. as well as support of the Academy of Sciences of the Czech Republic (grant number K 205 0602).

## Appendix A. The equivalence of Eqs. (13) and (14)

The exponent in Eq. (14) can, according to Eq. (6), be expressed:

$$\frac{1}{\Sigma} = \frac{2\sigma^2 B^2}{\beta^2} + 1 \quad (\text{A.1})$$

and Eq. (14) is then:

$$(\overline{M}_w/\overline{M}_n)_c = \exp \left[ \ln(\overline{M}_w/\overline{M}_n) \left( \frac{2\sigma^2 B^2}{\beta^2} + 1 \right) \right] \quad (\text{A.2})$$

which by substituting  $\ln \overline{M}_w/\overline{M}_n = \beta^2/2$  according to Eq. (2) gives:

$$(\overline{M}_w/\overline{M}_n)_c = \exp[\beta^2/2 + \sigma^2 B^2] \quad (\text{A.3})$$

and by substituting  $\beta^2/2$  from Eq. (2), Eq. (13) directly ensues.

## Appendix B. Derivation of Eq. (16)

Dividing Eq. (13) by Eq. (10), we have:

$$E = \frac{\sigma^2 \beta^2 + \sigma^4 B^2}{\sigma^2 + \beta^2/2B^2} \quad (\text{B.1})$$

where  $E$  is given by Eq. (17). Solving Eq. (B.1) for  $\sigma^2$ , we have:

$$\sigma^2 = \frac{E - \beta^2 + \sqrt{\beta^4 + E^2}}{2B^2} \quad (\text{B.2})$$

From Eqs. (12), (13) and (2) we have:

$$\beta^2 = \beta_c^2 - 2\sigma^2 B^2 \quad (\text{B.3})$$

Introducing Eq. (B.3) into Eq. (B.2) and denoting the  $i$ th approximation of  $\sigma^2$  by the subscript “ $i$ ”, i.e.  $\sigma_i \equiv \sigma$  Eq. (16) is obtained.

## References

- [1] A.E. Hamielec, *Pure Appl. Chem.* 54 (1982) 293.
- [2] A.E. Hamielec, A.C. Ouano, *J. Liq. Chromatogr.* 1 (1978) 111.
- [3] O. Procházka, P. Kratochvíl, *J. Appl. Polym. Sci.* 34 (1987) 2325.
- [4] M. Netopilík, *J. Chromatogr. A* 809 (1998) 1.
- [5] O. Procházka, P. Kratochvíl, *J. Appl. Polym. Sci.* 31 (1986) 919.
- [6] A.E. Hamielec, *J. Liq. Chromatogr.* 3 (1980) 381.
- [7] S. Mori, M. Ishikawa, *J. Liq. Chromatogr. Relat. Technol.* 21 (1998) 1107.
- [8] P.J. Wyatt, D.N. Villalpando, P. Alden, *J. Liq. Chromatogr. Relat. Technol.* 20 (1997) 2169.
- [9] W.W. Yau, *ACS Symp. Ser. (Chromatography of Polymers)* 731 (1999) 44.
- [10] M. Netopilík, *J. Chromatogr. A* 793 (1998) 21.
- [11] M. Bohdanecký, P. Kratochvíl, K. Šolc, *J. Polym. Sci., Part A* 3 (1965) 4153.
- [12] C. Jackson, *J. Chromatogr.* 645 (1993) 209.
- [13] P. Cheung, R. Lew, S.T. Balke, T.H. Mourey, *J. Appl. Polym. Sci.* 47 (1993) 1701.
- [14] M. Netopilík, *Polymer* 35 (1994) 4799.
- [15] C. Jackson, H.G. Barth, *Trends Polym. Sci.* 2 (1994) 203.
- [16] C. Jackson, *Polymer* 40 (1999) 3735.
- [17] M. Netopilík, *Polymer* 38 (1996) 127.
- [18] A.M. Kotliar, *J. Polym. Sci. A2* (1964) 4303.
- [19] L.H. Tung, *J. Appl. Polym. Sci.* 10 (1966) 375.
- [20] S. Vozka, M. Kubín, *J. Chromatogr.* 137 (1977) 225.
- [21] S.R. Lustig, *J. Chromatogr. A* 839 (1999) 1.
- [22] T.H. Mourey, S.T. Balke, *ACS Symp. Ser.* 521 (1993) 180.
- [23] P.J. Wyatt, *Anal. Chim. Acta* 272 (1993) 1.
- [24] P.J. Wyatt, *J. Chromatogr.* 648 (1993) 27.
- [25] D.W. Short, *J. Chromatogr. A* 686 (1994) 11.
- [26] P.J. Wyatt, L.A. Papazian, *Mag. Sep. Sci.* 11 (1993) 862.
- [27] M. Netopilík, *Polym. Bull.* 10 (1983) 478.
- [28] A.E. Hamielec, W.H. Ray, *J. Appl. Polym. Sci.* 13 (1969) 1319.
- [29] S.T. Balke, A.E. Hamielec, *J. Appl. Polym. Sci.* 13 (1969) 1381.
- [30] M. Netopilík, *Polymer* 38 (1997) 127.
- [31] G.V. Schulz, H. Baumann, *Makromol. Chem.* 114 (1968) 122.
- [32] J.R. Purdon, R.D. Mate, *J. Polym. Sci. Polym. Chem. Ed.* 6 (1968) 243.
- [33] M. Netopilík, *Int. J. Polym. Anal. Charact.* 6 (2001) 349.
- [34] M. Netopilík, Š. Podzimek, P. Kratochvíl, in preparation.
- [35] T.C. Kendrick, *J. Polym. Sci. A2* 7 (1969) 297.
- [36] S. Vozka, M. Kubín, *J. Polym. Sci.: Polym. Symp.* 68 (1980) 199.
- [37] J.J. Kirkland (Ed.), *Modern Practice of Liquid Chromatography*, Wiley Interscience, 1971.
- [38] P.J. Flory, *Principles of Polymer Chemistry*, Cornell University Press, Ithaca, New York, 1953.